An ab initio study on 3,4-methylenedioxymethamphetamine, MDMA (ecstasy) and its derivatives

Zahra Fallah Ebrahimi

Department of Chemical Engineering,
École Polytechnique de Montréal,
Montréal, QC H3T 1J4, Canada
Email: z.f.ebrahimi@gmail.com

Abstract: Computational studies have been carried out at DFT-B3LYP/ 6-31+G* and PW91P86/6-31+G* levels of theory on the structural and spectroscopic properties of 3,4-methylenedioxymethamphetamine (MDMA) and its derivatives. Nuclear quadrupole coupling constants (NQCCs) of ^{14}N and ^{17}O and chemical shift of ^{13}C and ^{1}H have been calculated. There is a good correlation between the calculated chemical shifts of ^{13}C and ^{1}H and experimental data. Our results showed that ^{14}N and ^{17}O NQCCs are quite sensitive to substitute-induced structural charge. In these compounds, a correlation has been observed between the parameters characteristic biological activity (LD50, IC50) and nuclear quadruple resonance (NQR) parameters. We also report a computational study for the ^{14}N and ^{17}O nuclear magnetic resonance (NMR) tensors in ecstasy and its derivatives. To our knowledge, no sufficient ab initio study has been carried out on MDMA and its derivatives.

Keywords: ab initio; 3,4-methylenedioxymethamphetamine; MDMA; NQCCs; nuclear quadrupole coupling constants; ecstasy; NMR; NQR; LD50; IC50.

Reference to this paper should be made as follows: Ebrahimi, Z.F. (2016) 'An ab initio study on 3,4-methylenedioxymethamphetamine, MDMA (ecstasy) and its derivatives', *Int. J. Computational Biology and Drug Design*, Vol. 9, Nos. 1/2, pp.149–161.

Biographical notes: Zahra Fallah Ebrahimi is doing her PhD at the École Polytechnique de Montréal University, Canada. In 2014, she obtained her DBA Program from Multimedia University, Malaysia. Her research interests are DFT, quantum chemistry, physical chemistry, MD, total quality management and SMEs.

1 Introduction

MDMA ($C_{11}H_{15}NO_2$), (3,4-methylenedioxymethamphetamine) (Figure 1) or what later became known as MDMA or Ecstasy, was first synthesised by Merck Pharmaceuticals in 1912 and investigated as an appetite suppressant. This drug induces a state of tranquil euphoria and since the late 1970s (Sull et al., 2003) has wide recreational use. 3,4 methylenedioxyamphetamine (MDA) and many N-substituted derivatives have also become drugs of abuse, which are being sold in tablet as 'Ecstasy'.

Figure 1 Derivatives of MDMA and the numbering scheme used for derivatives of methamphetamine (see online version for colours)

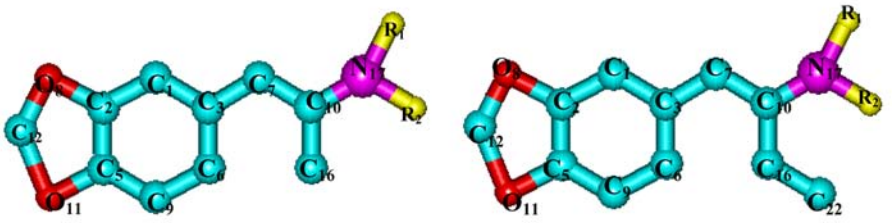

Group 1		Group 2	
MDA	R_1=R_2=H	MDP-2-B	R_1=R_2=H
MDMA	R_1=H, R_2=CH_3	MBDB	R_1=H, R_2=CH_3
MDEA	R_1=H, R_2=C_2H_5	EBDB	R_1=H, R_2=C_2H_5
MDMMA	R_1=R_2=CH_3	MDP-2-MMB	R_1=R_2=CH_3
NOHMDA	R_1=H, R_2=OH	MDP-2-OHB	R_1=H, R_2=OH

MDA: 3,4-methylenedioxyamphetamine
MDMA: 3,4-methylenedioxymethamphetamine
NOHMDA: N-hydroxy-1-(3,4-methylenedioxyamphetamine)
MDEA: 3,4-methylenedioxyethylamphetamine
MDMMA: N-methyl-1-(3,4-methylenedioxymethamphetamine)
MDP-2-MB (MBDB): N-methyl-1-(3,4-methylenedioxyphenyl)-2-butanamine
MDP-2-EB (EBDB): N-ethyl-1-(3,4-methylenedioxyphenyl)-2-butanamine
MDP-2-B: 3,4Methylenedioxyamphetamine
MDP-2-MMB: 3,4-methylenedioxy-N,Ndimethylamphetamine
MDP-2-OHB: N-hydroxy-3,4-methylenedioxyamphetamine

MDMA and its derivatives increase heart rate, blood pressure and myocardial oxygen consumption in both humans (Carvalho et al., 2004) and animals (Bexis and Docherty, 2006), which may ultimately result in tachycardia, hypertension, arrhythmias, cardiac ischaemia and hearing failure. More recently, MDMA has become more significant through their increasing use as a recreational drug among young people and serious cardiovascular damage. Although a number of studies investigated the behaviour, pharmacology (Green et al., 2003) and metabolism, but the effect of MDMA on the brain and its mechanism are not known completely.

Although the physical chemistry of MDMA has been poorly studied, Latasinska found a correlation between the parameters characterising biological activity and the NQR spectral parameters describing chemical properties of given compounds from a certain group. Wilson et al. (1988) studied MDMA and its derivatives using solid-state ^{13}C nuclear magnetic resonance and found that there is difference between solution and solid-state ^{13}C NMR spectra owing to main conformation deformation brought about by lattice packing. Morimoto et al. (1998) studied the structure of MDMA by single crystal X-ray. The terahertz (THz, far-infrared) spectrum of MDMA is simulated by utilising solid-state density functional theory (DFT) and it is identified that the isolated-molecule modes account for only half of the spectral features, but the remaining configuration arising from lattice vibrations cannot be forecasted because of the lack of solid-state molecular modelling (Allis et al., 2008). Results of Buchanan's studies (2010) show that the δ^2H values of MDMA-HCl are affected by the length of imine stir time, and the $\delta^{15}N$ values are affected by the degree of excess methylamine employed. Furthermore, the $\delta^{13}C$ and $\delta^{18}O$ values have been shown to be affected by the efficiency of the reaction, despite the similarity in C and O composition of the starting material and product molecules.

Furthermore, Buchanan et al. (2008) synthesised 18 MDMA samples from aliquots of the same precursor by three common reductive amination routes and analysed for ^{13}C, ^{15}N and ^{2}H isotope abundance using isotope ratio mass spectrometry (IRMS). It is identified that ^{2}H isotope abundance data is necessary for discrimination by synthetic route. Experimental studies by Liu et al. (2010) confirmed that ^{1}H NMR spectroscopy could present a suitable instrument for the rapid finding of MDMA in human urine. Lee et al. (2000) reported the differences in chemical shifts of the solid-state NMR and solution NMR for MDMA. This study described the differences between chemical shifts of MDMA-hydrochloric acid in ecstasy tablets and pure crystals. Experimental research by Heather et al. (2015) showed that the organic impurity profile of MDMA has been synthesised from catechol (1,2-dihydroxybenzene), a common chemical reagent available in industrial quantities.

The purpose of this paper is to present a theoretical study, ab initio, for the MDMA molecule and its derivatives to characterise the key parameters such as quadrupole coupling constant (QCC), NQR, chemical shift (δ), chemical shift anisotropy (CSA) and asymmetry parameters and also, to find a relationship between chemical structural and physical properties of these compounds and their biological activities.

Recently, much attention has been paid to look for a correlation between the physical and chemical properties such as dipolar moment or electron density distribution of compounds in these particular drugs and their biological activities (Latosinska, 2005). Some papers pay attention to find correlation between NQR data and biological activity (Latosinska et al., 2000).

2 Computational procedure

The quantum chemical calculations were carried out using GAUSSIAN 98 package (Frisch et al., 1998). All calculations are performed with the DFT with three parameter hybrid functional of Beek's B3, in which the local and non-local terms of the correlation functional are provided by LYP expression (Exner et al., 2012; Frank et al., 2012) in the 6-31G** and 6-31+G* standard basis sets. Prior to the DFT computations, the molecular geometries are optimised using PM3 semi-empirical method implemented in HyperChem software (HyperChem, 2002).

To evaluate the optimised structures of the molecules, frequency, a calculation is carried out using analytical second derivative and in all cases only real frequencies are obtained for the optimised structures.

The electric field gradient (EFG) and chemical shielding (CS) tensors components have been calculated at the same level of theory B3LYP for optimised geometry.

The gauge-included atomic orbital (GIAO) approach (Wolinski et al., 1990) is used in the CS tensor calculations. The principle CS tensor eigen values, δ_{11}, δ_{22} and δ_{33}, have the following relation:

$$\delta_{33} > \delta_{22} > \delta_{11}.$$

Chemical shielding anisotropy, $\Delta\delta$, is obtained by $\Delta\delta = \delta_{33} - (\delta_{22} + \delta_{11})/2$ (ppm). Chemical shielding isotropy, δ_{iso}, is obtained by $\delta_{iso} = (\delta_{11} + \delta_{22} + \delta_{33})/3$. To convert $^{15}N\delta_{iso}$, $^{13}C\delta_{iso}$ and $^{1}H\delta_{iso}$ to chemical shift isotropy, δ_{iso}, MDMA, with δ_{iso} (13C) = PPm and δ_{iso}(1H).

The principle EFG tensor eigen values, q_{xx}, q_{yy} and q_{zz}, have the following relation: $|q_{zz}| \rangle |q_{yy}| \rangle |q_{xx}|$. The NQCC, χ, is obtained by:

$$\chi = e^2 Q q_{zz} / h \text{ (MHz)},$$

where e is the charge of the electron, Q is the nuclear electric quadrupole moment of the nucleus and h is Planck's constant. Q values of ^{14}N, ^{2}H and ^{17}O, which are used in the calculation of χ values, have been reported by Pyykkö and Tokman (1997) as 20.44, 2.56 and 25.28 mb, respectively.

Another important parameter, which refers to the deviation of charge distribution from cylindrical symmetry, is the asymmetry parameter, η,

$$\eta = \left| \frac{q_{yy} - q_{xx}}{q_{zz}} \right|.$$

3 Results and discussion

3.1 Molecular structures

A selected set of the optimised geometrical parameters obtained for MDMA and its derivatives are listed in Table 1. The molecular structure and the numbering scheme used in this study for MDMA and its derivatives are demonstrated in Figure 1. These structural parameters show that the optimised geometry of MDMA is in excellent agreement with the solid-phase single crystal X-ray diffraction data (Morimoto et al., 1998). The substitution of ethyl with methyl at C_{10} and the N_{17}–C_{22} bond by similar amount of 0.021A. It was seen a comparable effect of the direction change in the N_{17}–C_{22} and C_{10}–N_{17}.

The other bond lengths, bond angles and torsion angle did not change significantly upon substitution of ethyl with methyl group and hydrogen group at C_{10} and N_{17}.

3.2 Natural bond orbital analysis

Table 2 presents the atomic charges of MDMA derivatives obtained by the natural bond orbital analysis (NBO). The largest change in the atomic charges of MDMA derivatives upon substitution has been observed at the nitrogen atoms.

The nitrogen charge decreased by ~0.5 and 0.2 upon the substitution of OH group and at N, respectively, because of the charge distributed upon substitution of alkyl group at the N.

The substitution at C_{10} did not change the charge at nitrogen significantly. The charge of the other atoms in MDMA remained approximately unchanged upon substitution at C_{10} and N_{17}.

3.3 IR frequencies and intensities

The absence of any imaginary frequency indicates that all of the optimised structures correspond to the minimum point on the intra-molecular potential energy surface. The frequency data of Table 3 contains important information about the relative strength of the corresponding bond in MDMA derivatives. The N–H stretching frequency

increases by about 58–122 cm^{-1} upon substitution of hydroxy group at N. These down shifts are attributed to in a N–H distance and acidity of the hydrogen atom in the N–H bond. But, the substitution of alkyl group at C_{10} increased the N–H stretching frequency or decreased the acidity of the hydrogen atoms.

Table 1 The optimised values of the bond length (in A°) and bond and dihedral angles (in degrees) obtained at the B3LYP method level of theory for ecstasy derivatives. 'Experimental data for MDMA (in HCL) given in parentheses'

	Group1					*Group2*				
Structure parameters	*MDMA*	*MDA*	*MDEA*	*MDMMA*	*NOHMDA*	*MBDB*	*MDP-2-B*	*MDP-2-MMB*	*EBDB*	*MDP-2-OHB*
$R(C_1\text{-}C_2)$	1.366 (1.374)	1.363	1.381	1.364	1.381	1.380	1.364	1.364	1.365	1.381
$R(O8\text{-}C_{12})$	1.408 (1.428)	1.406	1.438	1.407	1.438	1.438	1.406	1.407	1.408	1.439
$R(O_{11}\text{-}C_{12})$	1.407 (1.430)	1.407	1.437	1.407	1.438	1.438	1.407	1.407	1.408	1.439
$R(C_{10}\text{-}N_{17})$	1.456 (1.497)	1.457	1.491	1.462	1.498	1.493	1.457	1.461	1.461	1.502
$R(N_{17}\text{-}H_{26})$	1.001 (1.013)	1.002	0.999	–	0.994	0.998	1.001	–	1.016	0.995
$R(N_{17}\text{–}C_{22})$	1.447 (1.490)	–	1.485	1.446	–	1.473	–	1.443	1.451	–
			Bond	Angles	(in degree)					
$\angle C_{12}O_8C_2$	106.283 (105.75)	106.304	105.994	106.294	106.059	106.064	106.294	106.286	106.983	106.038
$\angle O_{11}C_{12}O_8$	107.414 (108.550)	107.443	108.842	107.446	108.769	108.809	107.445	107.451	107.741	108.748
$\angle O_{11}C_5C_2$	109.155 (109.450)	109.153	109.564	109.144	109.588	109.631	109.154	109.146	109.313	109.575
$\angle C_{12}O_{11}C_5$	106.192 (105.640)	106.144	106.032	106.158	106.045	105.991	106.133	106.155	106.842	106.056
$\angle N_{17}H_{26}C_{10}$	110.103 (106.330)	110.81	109.857	–	110.857	109.646	111.376	–	110.905	110.960
$\angle C_{10}N_{17}C_{22}$	116.339 (115.350)	–	114.364	114.985	–	114.810	–	117.252	116.560	–
			Torsion	Strain	(in degree)					
$\angle C_{12}O_{11}C_2C_5$	–8.376 (–3.53)	–8.717	–0.334	–8.668	–0.222	–0.295	–8.761	–8.656	–0.551	–0.009
$\angle C_{12}O_8C_2C_5$	8.261 (3.53)	8.718	0.343	8.612	0.070	0.213	8.751	8.575	0.476	–0.075
$\angle C_5O_{11}C_{12}O_8$	13.366 (6.090)	14.004	0.547	13.889	0.265	0.426	14.068	13.854	0.837	–0.038
			Bond	Length	(in A°)					

Table 2 The IGAIM calculated values of ^{13}C, ^{14}N NMR chemical shifts for the B3LYP/6-31+G* optimised structures of ecstasy derivatives (see Figure 2)

Charge	*MDMA*	*MDA*	*MDEA*	*MDMMA*	*NOHMDA*	*MBDB*	*MDP-2-B*	*MDP-2-MMB*	*MDP-2-OHB*	*EBDB*
C_1	–0.271	–0.262	–0.258	–0.256	–0.260	–0.261	–0.260	–0.259	–0.290	–0.263
C_2	0.259	0.257	0.256	0.256	0.257	0.263	0.257	0.255	0.256	0.255
C_7	–0.473	–0.466	–0.465	–0.468	–0.471	–0.465	–0.464	–0.466	–0.472	–0.466
O_8	–0.543	–0.544	–0.545	–0.545	–0.544	–0.546	–0.544	–0.545	–0.543	–0.544
C_{12}	0.209	0.210	0.210	0.210	0.209	0.211	0.209	0.210	0.209	0.2
N_{17}	–0.717	–0.918	–0.717	—0.564	–0.410	–0.719	–0.919	–0.577	–0.418	–0.722
C_{22}	–0.479	–	–0.267	-0.474	–	–0.680	–	–0.469	–	–0.269

Table 3 Selected harmonic frequencies γ (in cm^{-1}) computed at B3LYP/6-31+G* level of theory for derivatives of ecstasy (see Figure 1)

	Group 1					*Group 2*			
Mode	*MDMA*	*MDA*	*MDEA*	*MDMMA*	*NOHMDA*	*MBDB*	*MDP-2-B*	*MDP-2-MMB*	*EBDB*
γ_1	3497.78	3555.93	3480.11	–	3433.46	3528.0	3571.77	–	3524.87
γ_2	3099.23	3001.65	3097.46	3001.3	3097.54	3016.9	3097.13	3098.3	3002.52
γ_3	1068.92	1072.68	1072.67	975.1	1071.49	1067.6	1072.65	974.7	1073.35
γ_4	1168.83	–	3053.08	1269.6		1162.2	–	1320.1	2926.96

γ_1: stretching of N_{17}–H_{26} bond; γ_2: stretching of H–C_{12}–H bond; γ_3: stretching of C_{12}–O bond; γ_4: stretching of N_{17}–C_{22} bond.

The ring O–C–O stretching vibrations in the 974.7–1073.35 showed complex behaviour upon substitution at C_{10} and N_{17}. The γ_3 did change significantly upon substitution. This behaviour is in agreement with the unchanged C_{12}–O distances upon substitution (Table 3).

3.4 Chemical shielding tensors

The orientation of the principal values on the values of the molecular frame is critical to the chemical interpretation of the shift tensor values. This information has traditionally been obtained from either single crystal experiments or through dipolar correlation experiments.

However, in many cases, it is not possible to grow adequate single crystals, or, in the case of the liquid samples required to determine the orientation is quite difficult. In such cases, the theoretical techniques such as ab initio or DFT are very useful to obtain the chemical shielding tensors.

In this work, B3LYP and PW91P86 are the two levels of DFT and 6-31+G* are the standard basis set, which is reliable to calculate the oxygen, nitrogen and hydrogen CS tensors in the PAS that have been employed.

The calculated CS tensors have been reported as chemical shielding principle components, δ_{ij}, chemical shielding isotropy, δ_{iso}, and CSA, $\Delta\delta$, for ^1H, ^{15}N and ^{17}O for MDMA derivatives in Table 4.

Table 4 NQR calculation for ecstasy derivatives

Compounds		q_{xx}	q_{yy}	q_{zz}	η	χ
MDMA	O	0.003	1.663	–1.666	0.996	10.019
	N	–0.599	–0.513	1.112	0.077	5.343
	H	0.200	0.101	–0.359	0.437	0.241
MDA	O	0.002	1.665	–1.667	0.997	10.025
	N	–0.548	–0.439	0.988	0.110	4.747
	H	0.213	0.155	–0.386	0.148	0.259
MDEA	O	0.0001	1.667	–1.667	1.000	10.025
	N	–0.571	–0.530	1.101	0.037	5.290
	H	0.215	0.149	–0.364	0.181	0.245
MDMMA	O	–0.002	–1.666	1.668	0.997	10.031
	N	–0.609	–0.596	1.206	0.011	5.794
	H	–	–	–	–	–
NOHMDA	O	0.003	1.665	–1.667	0.997	10.025
	N	–1.183	–0.149	1.332	0.776	6.400
	H	0.202	0.147	–0.349	0.157	0.234
MBDB	O	0.002	1.665	–1.668	0.997	10.031
	N	–0.500	–0.594	1.094	0.086	5.252
	H	0.223	0.153	–0.376	0.186	0.253
EBDB	O	–0.005	1.663	–1.667	0.994	10.025
	N	–0.574	–0.508	1.082	0.061	5.199
	H	0.221	0.151	–0.372	0.188	0.249
MDP-2-B	O	0.001	1.665	–1.666	0.998	10.019
	N	–0.546	–0.440	0.986	0.107	4.737
	H	0.214	0.156	–0.369	0.157	0.248
MDP-2-MMB	O	–0.001	–1.666	1.667	0.998	10.025
	N	–0.640	–0.631	1.271	0.007	6.107
	H	–	–	–	–	–
MDP–2-OHB	O	0.002	1.664	–1.667	0.995	10.030
	N	–2.183	–0.049	1.433	0.886	6.500
	H	0.233	0.164	–0.366	0.150	0.263

Figures 2 and 3 display the correlation between the calculated and experimental chemical shift for ^{13}C and ^{1}H in MDMA derivatives, respectively. The results show a significant correlation between experimental data and data calculated from two levels.

The scatter is relatively larger for ^{1}H than those observed for ^{13}C chemical shift tensor. This result is consistent with the result observed in prior studies of uracil and benzamide when intermolecular effects are neglected in the calculations. It has been shown that inclusion of intermolecular interactions significantly improves the correlation between experimental and theoretical results.

Figure 2 Correlation between experimental data (C_{12}) and calculation data for MDMA, MDA (B3LYP/6-31+G*) and (PW91P86/6-31+G*) (see online version for colours)

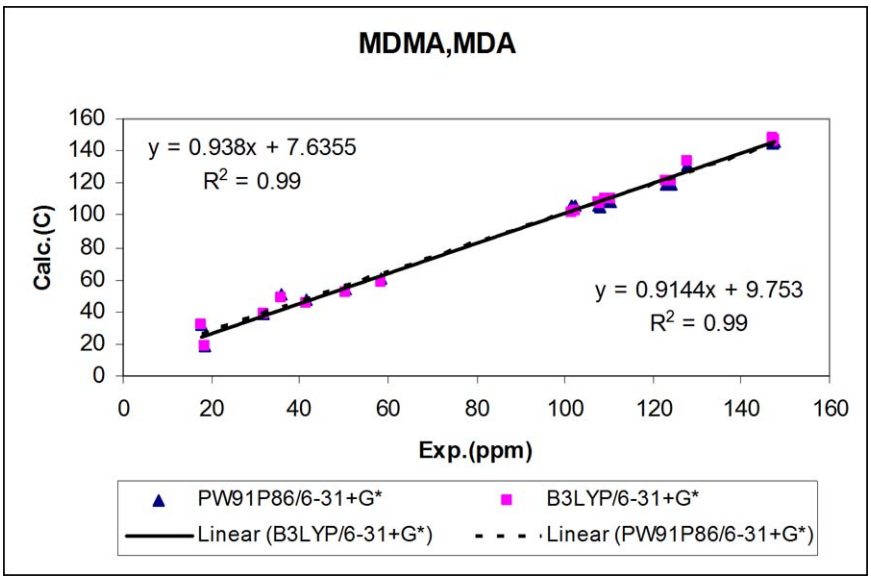

Figure 3 Correlation between experimental data(H) and calculation data for MBDB, EBDB (B3LYP/6-31+G*) and (PW91P86/6-31+G*) (see online version for colours)

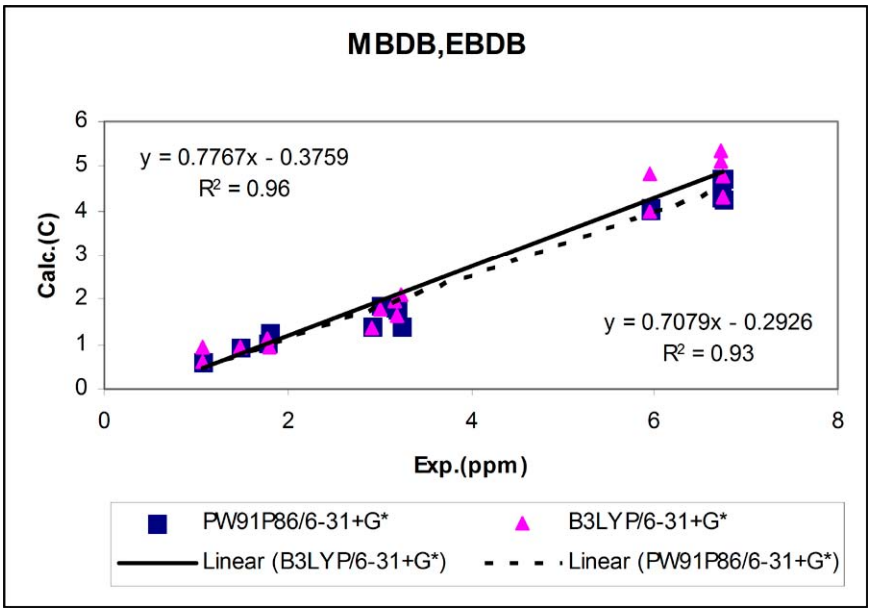

Since there are no experimental results for ^{15}N and ^{17}O chemical shift tensors in MDMA's derivatives in liquid or solid phase, the calculated values in Table 4 are constituted of theoretical predictions.

The substitution in C_{10} and N_{17} has different effects on chemical shift tensors of ^{15}N and ^{17}O in these derivatives. The results show that the isotropic chemical shift of ^{17}O is independent of the variation of the substitute and the tensor elements δ_{11}, δ_{22} and δ_{33} approximately remain constant. This is also possible that a priority of the direct (electronic) effect of substitution variation on the isotropic ^{17}O chemical shifts is small and its contribution to the isotropic ^{17}O chemical shifts could easily be masked by other local effects, e.g., neighbour anisotropy effects, slight changes in bond lengths and bond angles.

In contrast to the isotropic ^{17}O chemical shift, the isotropic ^{15}N chemical shift indeed inhibits modest dependencies on substitution variation. From the set of MDMA's derivatives in this study, one can see from Table 4 that isotropic ^{15}N chemical shift increased from 108.79 to 213.45 and 98.24 ppm with the substitution variation at C_{10} and N_{17} from hydroxy to hydrogen, respectively. This trend has been reported previously. Since δ_{iso} is noting more than a specific combination of the principle elements of the ^{15}N chemical shift tensor, other combination or individual elements might be expected to follow different trends.

It is identified that the substitution at C_{10} and N_{17} has direct effects on the electronic distribution around the nitrogen atom.

3.5 The electronic structure and biological activity

The correlated spectroscopic and quantum-mechanical research, reported in this work, has permitted a comprehensive analysis of the electron density distribution and identification of the reactive sites in amphetamine molecules.

Finally, it has been established that the biological activity of amphetamines is determined by the electron density distribution in N, which has been correlated from the results of the experimental study on metabolism of MDMA in human. The recent studies suggested that Phe120 companied in binding to MDMA. Also, a role for Phe120 in binding MDMA is supported by molecular dynamic calculations. Charge density effects on biological activity of amphetamines are due to the effect on binding of Phe120 to amphetamine, whereas the inductive effects modify it (decrease or increase the biological activity depending on the substitution being an electron donor or acceptor), and the density charge at N plays the most important role. According to Figures 4 and 5 with increasing IC_{50} or LD_{50} of amphetamines (corresponding to its decreasing biological activity), the quadrupole coupling constant of N increases. The same conclusions have been drawn of chemical shift.

As indicated by the results of a biological study, the strongest from among the amphetamines studies is MDA while the weakest is MBDB with electron donor group OH at N and ethyl at C10. The replacement by hydrogen and methyl in MDA significantly reduces its biological activity. It can be supposed to the most active site in amphetamines that is the N atom and this atom is playing the main role in the process of amphetamine bonding with Phe120.

3.6 NQR parameters

In this section, the calculated ^{17}O, ^{2}H and ^{14}N QCCs, χ, and asymmetry parameters, η, of MDMA's derivatives are discussed in Table 5. A look at the results reveals the influence

of substitution at C_{10} and N_{17} on the NQR parameters of oxygen atom can be neglected. This result is in agreement with the results obtained from the calculation of chemical shielding tensors. From the comparison of ^{14}N NQCC at different derivatives, we can find that ^{14}N χ value is shifted to higher values with a variation of substitution to: hydroxyl > two ethyl groups > ethyl > methyl > hydrogen.

Figure 4 Correlation between NQCC(N) and LD50 (see online version for colours)

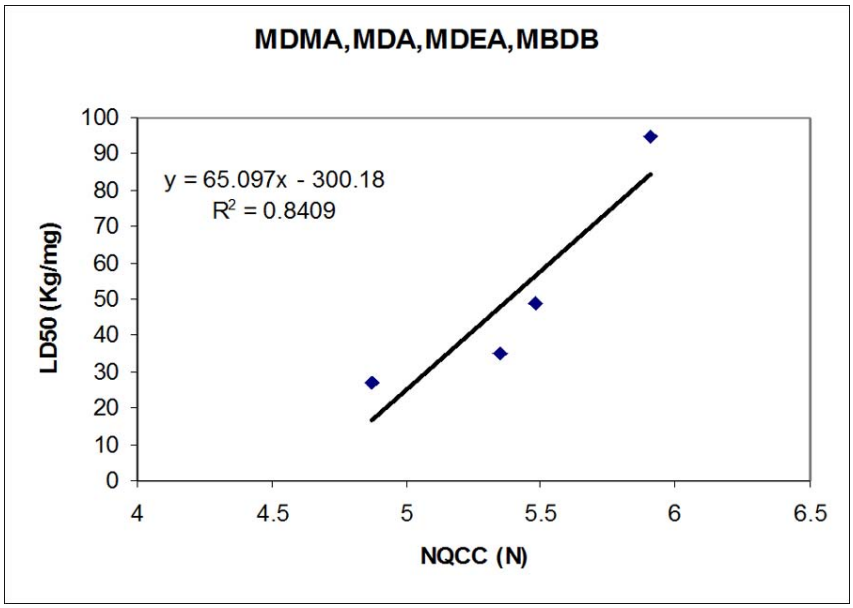

Figure 5 Correlation between NQCC(N) and IC50 (see online version for colours)

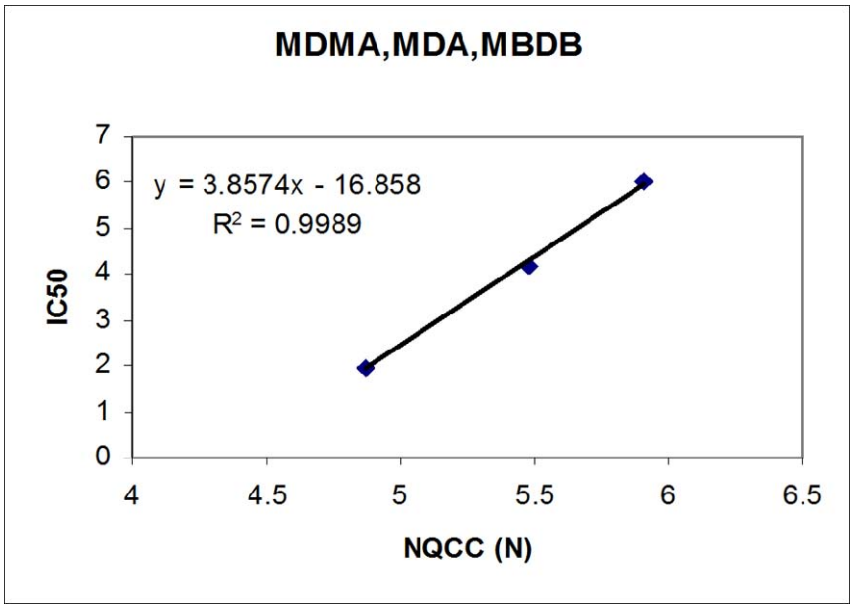

Table 5 Quantum chemical calculations of ^{15}N, ^{17}O chemical shift tensors with B3LYP/6-31+G*

Compound		*ppm*				
		δ_{iso}	δ_{11}	δ_{22}	δ_{33}	$\Delta\delta_{aniso}$
MDMA	O_8	200.505	151.628	175.826	247.062	110.335
	H_{26}	1.268	23.246	32.143	36.078	–3.782
	N_{17}	30.653	171.236	191.967	232.617	–26.013
MDA	O_7	200.413	151.224	176.334	273.681	109.901
	H_{26}	0.908	26.164	29.490	34.734	–2.305
	N_{17}	27.977	177.886	202.457	223.505	–8.332
EBDB	O_8	200.882	152.278	175.199	275.021	111.208
	H_{26}	0.976 (3.00)	23.304	32.128	35.157	–2.839
	N_{17}	36.427	148.636	207.633	222.228	–19.093
NOHMDA	O_8	200.893	151.762	176.292	274.67	110.599
	H_{26}	–2.711	22.555	25.993	30.994	–2.117
	N_{17}	131.017	19.468	80.190	195.071	–120.241
MDEA	O_{10}	201.047	152.410	176.404	274.327	109.921
	H_{25}	1.291	24.766	32.104	34.662	–1.624
	N_{12}	43.954	150.692	186.505	218.871	–25.273
MDP-2-B	O_8	200.394	151.185	176.569	273.429	109.552
	H_{26}	1.475	26.440	29.234	36.426	–3.977
	N_{17}	15.801	179.821	212.461	248.095	–26.954
MDMMA	O_7	201.483	153.137	176.634	274.675	109.789
	H_{26}	–	–	–	–	–
	N_{17}	2.097	193.815	241.299	246.373	–3.816
MDP-2-OHB	O_8	199.863	150.166	175.141	74.283	111.628
	H_{26}	–2.84	20.194	27.283	31.671	–3.330
	N_{17}	120.468	22.743	93.331	210.305	–127.268
MDP-2-MMB	O_8	201.271	152.795	176.329	274.688	110.126
	H_{26}	–	–	–	–	–
	N_{17}	–1.421	192.797	245.961	253.275	–8.896
MBDB	O_8	200.805	152.218	175.453	274.742	110.905
	H_{26}	0.975 (2.64)	22.772	31.192	36.624	–5.040
	N_{17}	19.629	172.154	211.006	245.733	–29.152

H NMR MDMA($N - CH_3$) = 2.7 (Calc. = 2.14), H NMR MDEA ($N - CH_2CH_3$) = 1.53 (Calc. = 1.24).

Moreover, the ^{14}N values show that the substitution of ethyl with methyl at C_{10} leads to a slight increase in by as much as 0.31 MHz when H is replaced by a hydroxyl group at the H site and η on this site increases noticeably as seen in Table 5. This is consistent with a much larger distortion of electron distribution around N because of the presence of the oxygen atom.

4 Conclusion

At the outset of this study, we optimise the geometry of MDMA and its derivatives and calculate the structural and spectroscopic properties at DFT-B3LYP/6-31+G* and PW91P86/6-31+G* levels. Results showed that ^{14}N and ^{17}O NQCC are quite sensitive to substitute-induced structural charge. In these compounds, a correlation has been observed between the parameters characteristic biological activity (LD50, IC50) and NQR parameters. Since the NQCC can be treated as descriptors QSAR, the information inferred from the NQR study on local electron density and charge distribution provides an excellent means for the determination of reactive sites and hence this can indicate a possible promising direction to be followed in drug design.

References

Allis, D.G., Hakey, P.M. and Korter, T.M. (2008) 'The solid-state terahertz spectrum of MDMA (Ecstasy) – a unique test for molecular modeling assignments', *Chemical Physics Letters*, Vol. 463, pp.353–356.

Bexis, S. and Docherty, J.R. (2006) 'Effects of MDMA, MDA and MDEA on blood pressure, heart rate, locomotor activity and body temperature in the rat involve A-adrenoceptors', *British Journal of Pharmacology*, Vol. 147, pp.926–934.

Buchanan, H.A., Daéid, N.N., Kerr, W.J., Carter, J.F. and Hill, J.C. (2010) 'Role of five synthetic reaction conditions on the stable isotopic composition of 3, 4-methylenedioxymethamphetamine', *Analytical Chemistry*, Vol. 82, pp.5484–5489.

Buchanan, H.A., Daéid, N.N., Meier-Augenstein, W., Kemp, H.F., Kerr, W.J. and Middleditch, M. (2008) 'Emerging use of isotope ratio mass spectrometry as a tool for discrimination of 3, 4-methylenedioxymethamphetamine by synthetic route', *Analytical Chemistry*, Vol. 80, pp.3350–3356.

Carvalho, M., Remiao, F., Milhazes, N., Borges, F., Fernandes, E., Monteiro, M.D., Goncalves, M.J., Seabra, V., Amado, F., Carvalho, F. and Bastos, M.L. (2004) 'Metabolism is required for the expression of ecstasy-induced cardiotoxicity in vitro', *Chemical Research in Toxicology*, Vol. 17, pp.623–632.

Exner, T.E., Frank, A., Onila, I. and Moeller, H.M. (2012) 'Toward the quantum chemical calculation of NMR chemical shifts of proteins. 3. Conformational sampling and explicit solvents model', *Journal of Chemical Theory and Computation*, Vol. 8, pp.4818–4827.

Frank, A., Moeller, H.M. and Exner, T.E. (2012) 'Toward the quantum chemical calculation of NMR chemical shifts of proteins. 2. Level of theory, basis set, and solvents model dependence', *Journal of Chemical Theory and Computation*, Vol. 8, pp.1480–1492.

Green, A.R., Mechan, A.O., Elliott, J.M., O'Shea, E. and Colado, M.I. (2003). 'The pharmacology and clinical pharmacology of 3, 4-Methylenedioxymethamphetamine (MDMA,'Ecstasy')', *Pharmacological Reviews*, Vol. 55, pp.463–508.

Heather, E., Shimmon, R. and Mcdonagh, A.M. (2015) 'Organic impurity profiling of 3, 4-methylenedioxymethamphetamine (MDMA) synthesised from catechol', *Forensic Science International*, Vol. 248, pp.140–147.

Hyperchem, R.F.W. (2002) *Molecular Modeling System: Hypercube*, http://www.hyper.com

Latosinska, J.N. (2005) 'Nuclear quadrupole resonance spectroscopy in studies of biologically active molecular systems – a review', *Journal of Pharmaceutical and Biomedical Analysis*, Vol. 38, pp.577–587.

Latosinska, J.N., Kasprzak, J. and Kazimierczuk, Z. (2000) 'Effects of chlorination and deoxiribose substitution on electron density distribution in indazole molecule studied by CL-35 NQR spectroscopy and ab initio calculations', *Journal of Molecular Structure-Theochem*, Vol. 530, pp.217–222.

Lee, G.S., Taylor, R.C., Dawson, M., Kannangara, G.K. and Wilson, M.A. (2000) 'High-resolution solid state 13 C nuclear magnetic resonance spectra of 3, 4-methylenedioxyamphetamine hydrochloride and related compounds and their mixtures with lactose', *Solid State Nuclear Magnetic Resonance*, Vol. 16, pp.225–237.

Liu, J., Decatur, J., Proni, G. and Champeil, E. (2010) 'Identification and quantitation of 3, 4-methylenedioxy-n-methylamphetamine (MDMA, ecstasy) in human urine by 1 H NMR spectroscopy. application to five cases of intoxication', *Forensic Science International*, Vol. 194, pp.103–107.

Frisch, M.J., Truks, G.W., Schlegel, H.B. Scuseria, G.E. Robb, M.A., Cheeseman, J.R., Zakrzewski, V.G., Montgomery Jr., J.A., Stratmann, R.E., Burant, J.C., Dapprich, S., Millam, J.M., Daniels, A.D., Kudin, K.N., Strain, M.C., Farkas, O., Tomasi, J., Barone, V., Cossi, M., Cammi, R., Mennucci, B., Pomelli, C., Adamo, C., Clifford, S., Ochterski, J., Petersson, G.A., Ayala, P.Y., Cui, Q., Morokuma, K., Malick, D.K., Rabuck, A.D., Raghavachari, K., Foresman, J.B., Cioslowski, J., Ortiz, J.V., Stefanov, B.B., Liu, G., Liashenko, A., Piskorz, P., Komaromi, I., Gomperts, R., Martin, R.L., Fox, D.J., Keith, T., Al-Laham, M.A., Peng, C.Y, Nanayakkara, A., Gonzalez, C., Challacombe, M., Gill, P.M.W., Johnson, B., Chen, W., Wong, M.W., Andres, J.L., Gonzalez, C. Head-Gordon, M., Replogle, E.S. and Pople, J.A. (1998) *Gaussian 98, Revision A.4*, Gaussian, Inc., Pittsburgh, PA.

Morimoto, B.H., Lovell, S. and Kahr, B. (1998) 'Ecstasy: 3, 4-methylenedioxymethamphetamine (MDMA)', *Acta Crystallographica Section C: Crystal Structure Communications*, Vol. 54, pp.229–231.

Pyykkö, P. and Tokman, M. (1997) *Determination of Nuclear Quadrupole Moments from High-Precision Atomic Calculations*, APS April Meeting Abstracts, p.1565.

Sull, T.J., Chass, G.A., Varro, A. and Papp, J.G. (2003) 'A comparative conformational analysis of selected central nervous system stimulants', *Journal of Molecular Structure-Theochem*, Vol. 623, pp.51–62.

Wilson, M.A. and Hatcher, P.G. (1988) 'Detection of tannins in modern and fossil barks and in plant residues by high-resolution solid-state 13 C nuclear magnetic resonance', *Organic Geochemistry*, Vol. 12, pp.539–546.

Wolinski, K., Hinton, J.F. and Pulay, P. (1990) 'Efficient implementation of the gauge-independent atomic orbital method for nmr chemical shift calculations', *Journal of the American Chemical Society*, Vol. 112, pp.8251–8260.